Chapter 22
Modeling Water Stress Effect on Soil Salinity

Gokmen Tayfur

Abstract As it is widely known the earth is experiencing a climate change. The primary effect of this change is the increase trend in global temperature. This, in turn, results in increased number of events in flooding, and drought in different parts of the world. A secondary effect is the change in water and soil salinity. A considerable portion of the cultivated land in the world is affected by salinity, limiting productivity potential. About 20 million ha of total 230 million ha of irrigated land in the world are salt affected. The climate change is expected to worsen this situation. This study explores the water stress effect on soil salinity. For this purpose, a model is developed to simulate salt transport in a layered soil column. The soil salinity transport model development involves two parts: (1) modeling salt movement through sail layers due to runoff, percolation, and lateral subsurface flow, and (2) modeling dissolution and precipitation of gypsum which acts as sink or source for salts in soil. The model is calibrated and validated with measured data. The soil is irrigated under optimal and water stress irrigation conditions. The major model parameters affecting the soil salinity are found to be wilting point, field capacity, hydraulic conductivity, initial soil salinity, and soil gypsum concentration. The results have revealed that water stress results in high concentration of salt accumulation in soil columns.

Keywords Modeling • Water stress • Salinity • Soil

22.1 Introduction

It is clearly known that the increasing of carbon dioxide and other greenhouse gases will raise global temperatures, resulting in global warming. This, in turn, will result in climate change which is expected to impact the world by affecting winter snow-

G. Tayfur (✉)
Department of Civil Engineering, Izmir Institute of Technology, Gulbahce Kampus, Urla, Izmir, Turkey
e-mail: gokmentayfur@iyte.edu.tr

A. Baba et al. (eds.), *Climate Change and its Effects on Water Resources*,
NATO Science for Peace and Security Series C: Environmental Security 3,
DOI 10.1007/978-94-007-1143-3_22,

fall and snowmelt, minimum water temperature, summer average temperature, and growing season rainfall amounts and intensities [1]. Temperature changes are expected to alter precipitation and evapotranspiration which are the prime drivers of water availability and agricultural production. Agriculture is an important economic activity in the world and the global warming is expected to have a great impact on water resources and agriculture [2].

Elgaalin and Garcia [2] investigated the impact of climate change on water supplies in Arkansas River Basin of Colorado under two transient climate change scenarios, employing artificial neural network method. Since monthly runoff is the primary factor in determining the amount of water available for irrigation, they linked the available potential water for agriculture to climate change on a monthly scale. They employed the two general circulation models (GCM) – HAD (Hadley Center for Climate Prediction and Research), and CCC (Canadian Climate Center) – to generate future climate projections assuming a progressively 1% annual increase in carbon dioxide concentrations [2]. Minville et al. [3] investigated the impact and uncertainty of climate change on water resources management in the Perobonka River System, Canada. They evaluated the impact of the change on medium-term reservoir operations for the Perobonka water resources system (Quebec, Canada) with annual and seasonal hydropower production indicators and flood control criteria.

Agricultural systems are more sensitive to the climate change due to the common lack of buffering capability in agricultural response to climate events. For example, a single month of extremely low rainfall may affect a reservoir by decreasing storage over the course of a few months, but the reservoir system might be able to recover quickly with single large rainfall. On the other hand, extremely low rainfall period of a month will cause death of a region's crops with no hope of growing new crops until next growing season. Hence, agricultural water resources planning must consider the variability in agricultural systems over time and the primary cause for temporal variation in climate [4].

Irrigation is a principal adaptation mechanism to climatic variability and economic studies have shown that climatic variability can be a factor in determining private investment in irrigation infrastructure more important than any others including credit availability, governmental price policies, and local violence [4]. Already irrigated agriculture takes place under water scarcity. This situation definitely will worsen in future. To cope with scarce supplies, deficit irrigation, i.e. application of water below full crop-water requirements, is an important tool to achieve the goal of reducing irrigation water use [5].

One of the major adverse effects of deficit irrigation, on the other hand, is the salinisation of the soil. Salinisation, which is also known as alkalisation or sodification, is the process that leads to an excessive increase of water-soluble salts in the soil. The accumulated salts include sodium, potassium, magnesium, calcium, chloride, sulphate, carbonate and bicarbonate that lead to severe deduction of soil fertility. Primary salinisation involves salt accumulation through natural processes due to a high salt content of the parent material or in groundwater. Secondary salinisation is caused by human interventions such as inappropriate irrigation practices, e.g. with salt-rich irrigation water and/or insufficient drainage. Salinisation is often associated with irrigated areas where low rainfall, high evapotranspiration rates or soil textural characteristics impede the washing out of the salts which subsequently build-up in the soil surface layers. Irrigation with high salt content waters dramatically worsens the problem.

Salinity is one of the most widespread soil degradation processes on the Earth. According to some estimates, the total area of salt affected soil is about one billion hectares. They occur mainly in the arid–semiarid regions of Asia, Australia and South America. In Europe, salt affected soil occurs in the Caspian Basin, the Ukraine, the Carpathian Basin and on the Iberian Peninsula. Soil salinity affects an estimated one million hectares in the European Union, mainly in the Mediterranean countries, and is a major cause of desertification. In Spain 3% of the 3.5 million hectares of irrigated land is severely affected, reducing markedly its agricultural potential while another 15% is under serious risk. The Euphrates, Tigris and Van basins are presenting an alarming situation with over 75,000 ha facing salinity-alkalinity problems [6]. Accordingly Kendirli et al. [7], 1.5 million ha of land in Turkey is salt effected and about 74% of barren land is saline soils.

The accumulation of salts, particularly sodium salts, is one the main physiological threats to ecosystems. Salt prevents, limits or disturbs the normal metabolism, water quality and nutrient uptake of plants and soil biota. When water containing a large amount of dissolved salt is brought into contact with a plant cell, the protoplasmic lining will shrink. This action, which is known as plasmolysis, increases with the concentration of the salt solution. The cell then collapses. In addition, sodium salts can be both corrosive and toxic to organic tissue. The nature of the salt, the plant species and even the individuality of the plant (e.g. structure and depth of the root system) determine the concentration of soil-salt levels at which a crop or plants will succumb. Examples of plants and crops with a high tolerance to salt include bermuda grass, cotton, date palm, peas, rape and sugar beet while apples, lemons, oranges, potatoes and most clovers have a very low tolerance.

Salinization processes are near to irreversible in the case of heavy-textured soils with high levels of swelling clay. Although a combination of efficient drainage and flushing of the soil by water is often used, the leaching of salts from the profile is rarely effective. Because the reclamation, improvement and management of salt affected soils necessitate complex and expensive technologies, all efforts must be taken for the efficient prevention of these harmful processes. Permanent care and proper control actions are required. Adequate soil and water conservation practices, based on a comprehensive soil or land degradation assessment, can provide an "early warning system" that provides possibilities for efficient salinity control, the prevention of these environmental stresses and their undesirable ecological, economical and social consequences.

This study presents a mathematical model for simulating salt transport in saturated/unsaturated soil. The effect of deficit irrigation on the salt accumulation in the soil column is quantitatively investigated and tested against measured data.

22.2 Salt Transport Model

The model simulates salt transport downward and upward. Downward movement involves two parts – (1) modeling movement in the top layer of 10 cm thickness; and (2) modeling the movement under the layers below the top layer (Fig. 22.1). In the top layer, total water flow leaving the surface layer consists of rainfall, lateral subsurface flow, and vertical percolation (Fig. 22.2). In other soil layers, the total water flow consists of only lateral subsurface flow and vertical percolation (Fig. 22.3).

The downward salt movement can be formulated as follows [8]:

$$S = S_i \left[1 - \exp\left(\frac{-W_t}{n - \theta_w} \right) \right] \tag{22.1}$$

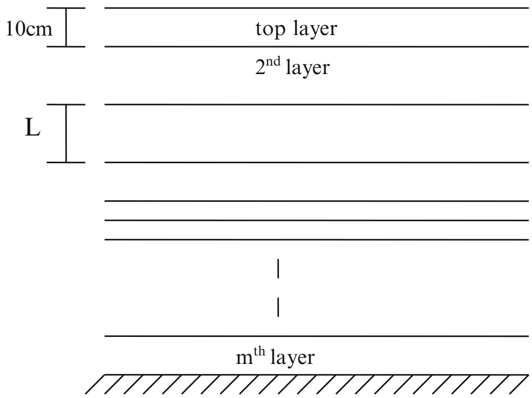

Fig. 22.1 Schematic representation of layers in a soil column

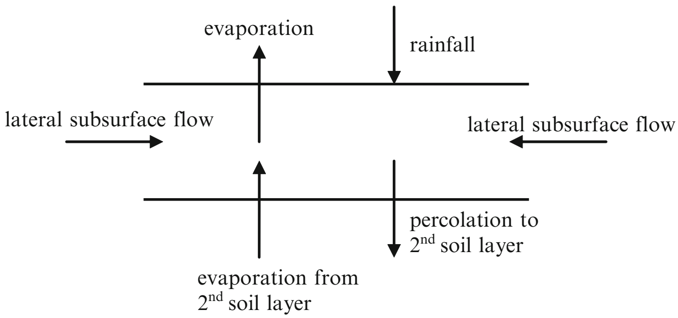

Fig. 22.2 Schematic representation of flow and evaporation mass transport in the top soil layer

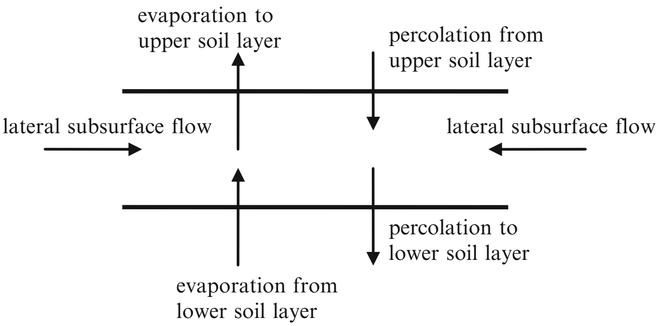

Fig. 22.3 Schematic representation of flow and evaporation mass transport in an inner soil layer

where S is salt mass in total water flow, S_i is initial salt mass in the soil layer; W_t is total water flow, n is soil porosity, and θ_w is the wilting point water content. The final salt mass contained in the soil layer is expressed as $S_f = S_i - S$ and the average salt concentration is expressed as $C_s = S/W$ where C_s is the average salt concentration associated with the total water flow. Hence, salt mass contained in runoff, lateral flow, and percolation is found by the product of corresponding water flow and salt concentration.

The upward salt movement is due to water evaporation from the spoil. When water is evaporated from the soil surface, salt is moved upwards into the top soil layer by mass flow. The equation for estimating this salt transport is expressed as [8]:

$$S_{ev} = \sum_{l=2}^{m} E_{vl} C_{sl} \tag{22.2}$$

where S_{vl} is salt mass moved from lower layers to top layer by soil water evaporation and E_{vl} stands for soil water evaporation amount in the contributing layers. Subscription l refers to soil layer and m represents the number of layers contributing to soil water evaporation.

Other major source of salt in a soil column comes from gypsum dissolution. The time dependent gypsum dissolution is defined by Kemper et al. [9] as:

$$\frac{dC_g}{dt} = K_d (C_{gs} - C_g) \tag{22.3}$$

where C_g is solution concentration at any time, C_{gs} is solution concentration at gypsum saturation which is taken as 4% (g of gypsum/g of soil) or 2.63 g/L in soil solution [10] and K_d is the dissolution coefficient.

Integrating Eq. 22.3 from $t = 0$ (water enters the soil layer) to $t = t_c$ (water leaves the soil layer) yields $K_d t_c = ln(C_g/C_{gs} - 1)$. Keren and O'Connor [11] conducted a gypsum dissolution study using soil samples amended with 2% and 4% gypsum under different water flow velocities and concluded that $K_d t_c = \alpha t_c^{0.5} + \beta$ where α and β are coefficients. According to Kemper et al. [9], $t_c = L/W$ where L is thickness of soil layer and W is actual flow velocity which is the Darcy velocity divided by the porosity. Assuming that soil porosity is equal to the saturated soil moisture content (θ_s) [12], the dissolution coefficient can be expressed as:

$$K_d = \alpha\sqrt{\frac{W}{L\theta_s}} + \beta\left(\frac{W}{L\theta_s}\right) \tag{22.4}$$

Hence, gypsum dissolution at any time can be computed as [12]

$$C_g(t) = K_d(t)\theta(t)C_g(t-1) \tag{22.5}$$

where t and $(t-1)$ stand for present and previous time steps, respectively, and θ is soil moisture content. The dissolved gypsum mass is the product of $C_g(t)$ and water flux, W. The values of the α and β coefficients obtained by Keren and O'Connor [11] are as follows:

$$\begin{aligned} &\alpha = 1.2h^{-0.5} \\ &\beta = 0.0 \end{aligned} \qquad \text{for } 0\% \le gypsum \le 2\%$$

$$\begin{aligned} &\alpha = 2.55h^{-0.5} \\ &\beta = 0.0 \end{aligned} \qquad \text{for } 2\% < gypsum \le 4\%$$

Gypsum precipitation due to the soil water evaporation can be expressed as [8]:

$$G_p = \sum_{l=2}^{m} E_{vl}C_{gl} \tag{22.6}$$

where G_p is the mass of calcium and sulfate ions that are evapoconcentrated and precipitated back to gypsum as a result of the soil water evaporation from lower layers towards top layer.

The total salt mass balance at any soil layer (l) can then be expressed as [8]:

$$T_{sl} = S_{il} - (S_l + G_{dl}) + (S_{evl} + G_{pl}) \tag{22.7}$$

where T_{sl} and S_{il} are final and initial salt mass in a soil layer l, respectively. S_l is salt mass lost from soil layer l due to total water flow leaving the layer. G_{dl} is mass of dissolved components (calcium and sulfate ions) of gypsum lost from soil layer l due to the total water flow leaving the layer. S_{evl} *is* salt mass moved to the layer l from contributing lower layers due to soil water evaporation. G_{pl} is mass of precipitated components (calcium and sulfate ions) of gypsum moved to the soil layer l due to the soil water evaporation. The total salt mass, Tsl (t/ha) and soil saturation extract Ece (dS/m) in a soil layer l can be expressed as [8]:

$$T_{sl}\left(t/ha\right) = EC_e \cdot 640\,(g/m^3) \cdot \theta \cdot L(m) \cdot 1x10^4(m^2/ha) \cdot 1x10^{-6}(g/t) \tag{22.8}$$

where L is the thickness of a soil layer l (see Fig. 22.1).

22.3 Model Calibration and Validation

The model is calibrated and validated with soil EC_e data obtained by Champion et al. [14] at the Fruita Research Center in Grand Valley in Coloroda. The soil in the Center contains gypsum and soluble salts. The topsoil thickness is 74 cm of loam and sandy loam. The underlying material to a depth of 150 cm is stratified loamy fine sand, silt loam, silty clay loam and very fine sandy loam. The experimental site contained six lysimeters of 1.55 × 1.22 × 1.22 m deep. The weather data consists of daily maximum, minimum temperatures, solar radiation, wind speed, and precipitation. The soil data consists of soil moisture and ECe and the irrigation data contained the dates and rates of applied water. The lysimeters were surface irrigated with water from Colorado River having an average ECe of 0.65 dS/m. Alfalfa was grown in the lysimeters. The lysimeters were applied a total of 796 mm irrigation water from April 15 to September 23, 1986.

Data from one of the lysimeters is used for the model calibration. Table 22.1 shows the measured versus predicted ECe values in time along a soil depth. The computed mean absolute error (MAE) and mean relative error (MRE) for the results in Table 22.1 are, respectively, 1.17 dS/m and 34.9%. Table 22.2 shows the calibrated values of the model parameters that resulted in the simulations summarized in Table 22.1. The calibrated model was then applied to simulate salt variation in a soil column experiment of the same lysimeter in Fruita Research Center in

Table 22.1 Measured versus predicted ECe values as a result of the calibration procedure

Soil layer depth (cm)	Measured ECe (dS/m)	Predicted ECe (dS/m)	Date
1.17	30.0	1.00	May 23, 1986
1.69	60.0	4.26	
7.12	90.0	6.23	
1.20	30.0	1.00	June 12, 1986
1.72	60.0	3.25	
7.05	90.0	6.75	
1.38	30.0	1.50	September 9, 1986
1.72	60.0	3.30	
6.55	90.0	3.35	

Table 22.2 Parameter values as a result of the calibration procedure

	Soil layer depth (cm)		
Parameter	0–30	30–60	60–90
Wilting point water content	0.116	0.120	0.059
Field capacity	0.398	0.418	0.359
Saturated conductivity (mm/h)	2.500	5.500	8.200
Initial gypsum concentration (mg/L)	1.100	4.600	8.800
Initial measured ECe (dS/m)	8.850	8.850	8.850

Table 22.3 Measured versus predicted ECe values as a result of the validation procedure

Date	Measured ECe (dS/m)	Predicted ECe (dS/m)
March 10, 1988	3.05	3.05
March 25, 1988	4.60	4.70
April 10, 1988	4.82	4.65
April 25, 1988	5.00	4.75
May 10, 1988	5.70	5.10
September 30, 1988	3.25	4.85

1988. Alfalfa in the same lysimeter received about 841 mm irrigation rate from April 20 to September 16, 1988. Table 22.3 shows the validation model results in predicting ECe in time in the 90 cm soil profile. The computed MAE = 0.45 dS/m and MAE = 11.7 implying satisfactory performance of the model.

22.4 Water Stress Effects on Salt Movement

The effect of irrigation water stress that is already seen in some parts the world as a result of water shortage and it will surely be employed in near future in most part of the world due to global warming effects is investigated in this study. The calibrated and validated salt transport model, in order to see the effects of the water stress on salt transport, is applied to a 1992 study of Robinson et al. at the Desert Research and Extension Center, University of California, in the Imperial Valley of California. Table 22.4 presents four different irrigation treatment – optimum check, minimum stress, short stress, and long stress. The irrigation water which is diverted from Colorado River into All American Canal had an average ECw of 1.25 dS/m (850 mg/L) about twice of the one used at the Fruite Research Center, CO. The soil in the Imperial Valley is Holtville clay extending 60–90 cm in depth overlying sandy clay. The observed ECe in 1991 was assumed as initial ECe values.

Table 22.5 summarizes observed versus predicted salt concentrations along the soil depth of 120 cm. The measured salt concentration data clearly show that under stress conditions, salt concentration increases along the soil depth in time. For example, in between 60 and 120 cm zone, on the average, the measured ECe on October 16, 1991 was around 6.08 dS/m under optimum conditions, it then became 6.93 under minimum stress, 8.38 under short stress, and 9.88 dS/m under long stress conditions. The salt concentration increase is, on the average, 14%, 38%, and 63% under minimum, short, and long stress conditions, respectively. The results in the table show that the developed salt transport model shows good performance in predicting concentrations under optimum and minimum stress conditions along the soil depth. Under short and long stress conditions, the model performs poorly in predicting salt concentrations especially in the lower zone. The computed error measures, on the average, for the results in Table 22.5 are MAE = 1.15 dS/m and MRE = 25.4%.

Table 22.4 Water stress irrigation treatments in 1991 in the Imperial Valley, CA

	Number of total applied type irrigations water				
Treatment type	July	August	September	October	
Optimum	3	2	2	2	1,269
Minimum stress	3	1	1	2	1,203
Short stress	3	0	0	2	991
Long stress	0	0	0	2	821

Table 22.5 Measured versus predicted ECe values under four different stress conditions

Date	Soil layer depth (cm)	Measured ECe (dS/m)	Predicted (dS/m)
Optimum treatment			
June 4, 1986	30.0	2.60	4.10
	60.0	3.30	3.95
	90.0	6.40	5.75
	120.0	5.85	5.70
September 4, 1986	30.0	2.90	4.85
	60.0	3.40	4.40
	90.0	6.95	5.75
	120.0	5.90	5.70
October 16, 1986	30.0	3.20	5.05
	60.0	3.45	4.55
	90.0	6.30	6.90
	120.0	5.85	5.70
Minimum stress treatment			
June 4, 1986	30.0	2.30	3.55
	60.0	3.20	3.45
	90.0	6.30	6.55
	120.0	6.90	7.10
September 4, 1986	30.0	2.55	4.10
	60.0	3.90	3.80
	90.0	6.60	6.60
	120.0	6.85	7.10
October 16, 1986	30.0	2.65	4.55
	60.0	4.55	4.00
	90.0	7.45	6.60
	120.0	6.40	7.00
Short stress treatment			
June 4, 1986	30.0	2.55	4.10
	60.0	4.75	4.35
	90.0	7.05	6.10
	120.0	6.10	6.30
September 4, 1986	30.0	2.80	4.15
	60.0	5.40	4.45
	90.0	8.70	6.00
	120.0	5.75	6.10

(continued)

Table 22.5 (continued)

Date	Soil layer depth (cm)	Measured ECe (dS/m)	Predicted (dS/m)
October 16, 1986	30.0	3.00	5.00
	60.0	5.50	4.35
	90.0	10.20	6.00
	120.0	6.55	6.20
Long stress treatment			
June 4, 1986	30.0	2.20	3.68
	60.0	3.20	3.70
	90.0	5.65	5.45
	120.0	6.30	6.32
September 4, 1986	30.0	2.45	3.55
	60.0	3.75	3.70
	90.0	9.25	4.74
	120.0	8.95	6.25
October 16, 1986	30.0	2.75	4.05
	60.0	4.05	3.80
	90.0	10.80	5.20
	120.0	8.95	6.50

22.5 Concluding Remarks

Climate change as a result of global warming will have a deep impact on surface and groundwater systems and, as a result, on the agriculture which is very responsive the climate change in a very short period time. Irrigation is a way of adaptation to the climate change and the deficit irrigation is a practical tool for the adaptation. However, the impact of such management results in salt accumulation in the soil zone reduces the fertility of the soil, as presented in this study. The reclamation of such soils is very expensive and requires complex technology. It is therefore essential to find a balance between deficit irrigation and its consequence of salt accumulation. The model measured results show that long stress treatment is not a viable solution. Short stress treatment is a delicate. Minimum stress treatment can be confidently employed. The transport model can satisfactorily simulate salt transport under optimum and minimum stress conditions. However, it does not perform well in predicting the concentrations in prolonged stress periods especially in the lower zones. Hence, the model should be improved to overcome this shortcoming or it should be used with care for the stress periods.

References

1. Baron JS, Hartman MD, Kittle TGF, Brand LE, Ojima DS, Lammers RB (1998) Effects of land cover, water redistribution, and temperature on ecosystem processes in the South Platte Basin. Ecol Appl 8(4):1037–1051

2. Elgaali E, Garcia LA (2007) Using neural networks to model the impacts of climate change on water supplies. J Water Res Pl 133(3):230–243
3. Minville M, Brissette F, Leconte R (2010) Impacts and uncertainty of climate change on water resources management of the Peribonka River system (Canada). J Water Res Pl 136(3):376–385
4. Brumbelow K, Georgakakos A (2007) Consideration of climate variability and change in agricultural water resources planning. J Water Res Pl 133(3):275–285
5. Fereres E, Soriano MA (2007) Deficit irrigation for reducing agricultural water use. J Exp Bot 58(2):147–159
6. Ozturk M, Ozcelik H, Sakcali S, Guvensen A (2004) Land degradation problems in the Euphrates Basin, Turkey. Int Soc Environ Bot, EnviroNews Arch 10(3):7–9
7. Kendirli B, Cakmak B, Ucar Y (2005) Salinity in the Southeastern Anatolia Project (GAP), Turkey: issues and options. Irrig Drainage 54:115–122
8. Tayfur GN, Tanji KK, House B, Robinson F, Teuber L, Kruse G (1995) Modeling deficit irrigation in alfalfa production. J Irrig Drain E 121(6):442–451
9. Kemper WD, Olsen J, de Mooy CR (1975) Dissolution rate of gypsum in flowing water. Soil Sci Soc Am Proc 39:458–463
10. Karajeh FF (1991) A numerical model for management of subsurface drainage in agroforestry systems. PhD dissertation, University of California, Davis
11. Keren R, O'Connor GA (1982) Gypsum dissolution and sodic soil reclamation as affected by water flow velocity. Soil Sci Soc Am Proc 46:726–732
12. Karajeh FF, Tanji KK (1994) Agroforestry drainage management model III. Field salt flow. J Irrig Drain E 120(2):397–413
13. Robinson EF, Teuber LR, Loomis SR (1992) Alfalfa water stress management during summer months in Imperial Valley for water conservation. Annual report to Metropolitan Water District of Southern California, Water Resources Center, UC, and Imperial Valley Conservation Research Center Committee, UC Desert Research Center and Extension Center, El Centro
14. Champion DF, Kruse EG, Olsen SR, Kincaid DC (1991) Salt movement under level-basin irrigation. J Irrig Drain E 117(5):642–655